2018

Watershed-Scale Drivers of Air-Water CO2 Exchanges in Two Lagoonal North Carolina (USA) Estuaries

Bryce R. Van Dam
University of North Carolina at Chapel Hill

Joseph R. Crosswell
Virginia Institute of Marine Science

Iris C. Anderson
Virginia Institute of Marine Science

Hans W. Paerl
University of North Carolina at Chapel Hill

AGU PUBLICATIONS

JGR

Journal of Geophysical Research: Biogeosciences

RESEARCH ARTICLE
10.1002/2017JG004243

Key Points:
- We identify a zone of minimum pCO_2 when freshwater age is approximately 2-3 weeks, for marine- and river-dominated estuaries alike
- CO_2 flux is largely supported by autochthonous CO_2 in a marine-dominated estuary but by riverine inputs in a nearby river-dominated estuary
- Differences in carbonate buffering suggest that both estuaries are uniquely sensitive to acidification stress from additional CO_2 inputs

Supporting Information:
- Data Set S1
- Supporting Information S1

Correspondence to:
B. R. Van Dam,
bvandam@live.unc.edu

Citation:
Van Dam, B. R., Crosswell, J. R., Anderson, I. C., & Paerl, H. W. (2018). Watershed-scale drivers of air-water CO_2 exchanges in two lagoonal North Carolina (USA) estuaries. *Journal of Geophysical Research: Biogeosciences*, *123*, 271–287. https://doi.org/10.1002/2017JG004243

Received 23 OCT 2017
Accepted 4 JAN 2018
Accepted article online 9 JAN 2018
Published online 30 JAN 2018

Watershed-Scale Drivers of Air-Water CO_2 Exchanges in Two Lagoonal North Carolina (USA) Estuaries

Bryce R. Van Dam[1], Joseph R. Crosswell[1,2,3], Iris C. Anderson[3], and Hans W. Paerl[1]

[1]Institute of Marine Sciences, University of North Carolina at Chapel Hill, Morehead City, NC, USA, [2]CSIRO Oceans and Atmosphere, Brisbane, Queensland, Australia, [3]Virginia Institute of Marine Science, College of William and Mary, Gloucester Point, VA, USA

Abstract Riverine loading of nutrients and organic matter act in concert to modulate CO_2 fluxes in estuaries, yet quantitative relationships between these factors remain poorly defined. This study explored watershed-scale mechanisms responsible for the relatively low CO_2 fluxes observed in two microtidal, lagoonal estuaries. Air-water CO_2 fluxes were quantified with 74 high-resolution spatial surveys in the neighboring New River Estuary (NewRE) and Neuse River Estuary (NeuseRE), North Carolina, which experience a common climatology but differ in marine versus riverine influence. Annually, both estuaries were relatively small sources of CO_2 to the atmosphere, 12.5 and 16.3 mmol C m^{-2} d^{-1} in the NeuseRE and NewRE, respectively. Large-scale pCO_2 variations were driven by changes in freshwater age, which modulates nutrient and organic carbon supply and phytoplankton flushing. Greatest pCO_2 undersaturation was observed at intermediate freshwater ages, between 2 and 3 weeks. Biological controls on CO_2 fluxes were obscured by variable inputs of river-borne CO_2, which drove CO_2 degassing in the river-dominated NeuseRE. Internally produced CO_2 exceeded river-borne CO_2 in the marine-dominated NewRE, suggesting that net ecosystem heterotrophy, rather than riverine inputs, drove CO_2 fluxes in this system. Variations in riverine alkalinity and inorganic carbon loading caused zones of minimum buffering capacity to occur at different locations in each estuary, enhancing the sensitivity of estuarine inorganic C chemistry to acidification. Although annual CO_2 fluxes were similar between systems, watershed-specific hydrologic factors led to disparate controls on internal carbonate chemistry, which can influence ecosystem biogeochemical cycling, trophic state, and response to future perturbations.

Plain Language Summary Estuaries release nearly as much CO_2 to the atmosphere as is taken up over the continental shelf. However, estuarine emissions vary greatly across space and time, contributing significantly to the uncertainty of global carbon budgets. In this study, we assess spatial and temporal variability in CO_2 emissions from adjacent estuaries in North Carolina, USA. These emissions varied across seasons and river discharge conditions but were relatively small when assessed as annual averages. Freshwater age (time freshwater spends in estuary before being flushed to ocean) was an important driver of CO_2 dynamics in both estuaries, due to its role in regulating nutrient, DOC, and DIC supply while also affecting the rate at which phytoplankton are flushed from the system. While the relationship between freshwater age and CO_2 was similar for both estuaries, we show that the various external and internal inputs of CO_2 were quite different. Riverine CO_2 inputs drove CO_2 emissions in the river-dominated estuary, while internally produced CO_2 (from community respiration) was more important in the marine-dominated estuary. We also demonstrate that poorly buffered regions in both estuaries are particularly vulnerable to acidification, with potentially negative impacts on calcifying organisms.

1. Introduction

Estuaries are important biogeochemical and trophic links between terrestrial and marine systems and provide critical ecosystem services to coastal populations (Hobbie, 2000; Pendleton, 2008; Wetz & Yoskowitz, 2013). Estuaries often receive large allochthonous organic matter loads, which support high remineralization rates and drive them toward net ecosystem heterotrophy and CO_2 degassing (Bauer et al., 2013; Borges & Abril, 2011; Cai, 2011; Frankignoulle et al., 1998). At the same time, nutrients (nitrogen and phosphorus) supplied externally or recycled internally drive high rates of autochthonous organic matter production in these ecosystems, causing some estuaries to act as CO_2 sinks (Crosswell et al., 2012, 2017; Drupp et al., 2011; Hunt et al, 2011; Maher & Eyre, 2012). The balance between these factors varies over space and time, making it

difficult to globally integrate CO_2 fluxes across these diverse ecosystems. Early attempts at scaling estuarine CO_2 fluxes globally or regionally resulted in relatively high estimates, on the order of 100–500 mmol C m^{-2} d^{-1} (Borges, Delille, et al., 2004; Borges, Vanderborght, et al., 2004; Frankignoulle et al., 1998), which have since been revised downward by an order of magnitude (Cai, 2011; Chen & Borges, 2009; Laruelle et al., 2010, 2013; Maher & Eyre, 2012; Regnier et al., 2013). This decrease was largely due to the inclusion of microtidal and marine-dominated systems, which are relatively small sources of CO_2 to the atmosphere (Jiang et al., 2008), and as a result, the most recent globally scaled estimates of estuarine CO_2 degassing have again decreased, to ~20–40 mmol C m^{-2} d^{-1} (Laruelle et al., 2013; Maher & Eyre, 2012; Regnier et al., 2013). Because microtidal, lagoonal estuaries make up ~50% of the global estuarine surface area (Chen et al., 2013; Crosswell et al., 2012; Kennish & Paerl, 2010; Laruelle et al., 2013), information on the drivers of air-water CO_2 exchange across the diverse range of such systems is needed if we are to accurately scale this biogeochemical flux globally.

In microtidal, lagoonal estuaries, variations in the timing and magnitude of river discharge regulate nutrient supply as well as the quality and quantity of organic matter (Crosswell et al., 2012; Koné et al., 2009; Mallin et al., 1993; Paerl et al., 2014). Hence, the metabolic balance of a given estuary is closely linked to the hydrology of its watershed. This idea is supported by previous findings linking seasonal to annual variation in CO_2 flux with changes in freshwater delivery, through both surface (Akhand et al., 2016; Drupp et al., 2011; Flecha et al., 2015; Guo et al., 2009; Yao et al., 2007; Zhai et al., 2005) and groundwater channels (Call et al., 2015; Jeffrey et al., 2016; Macklin et al., 2014; Santos et al., 2010). Watershed-scale hydrology may also drive complex changes in the buffering capacity of estuarine waters, impacting calcifying organisms (Barton et al., 2012; Hofmann et al., 2010), pH-sensitive processes like nitrification (Beman et al., 2010; Huesemann et al., 2002), and even animal behavior (Dodd et al., 2015; Leung et al., 2015). While ocean acidification has caused a variable but generally negative impact on calcifying phytoplankton and benthic invertebrates (Doney et al., 2009; Hofmann et al., 2010), elevated atmospheric CO_2 may actually enhance the productivity of C3-dominated salt marshes (Langley & Megonigal, 2010; Mozdzer & Megonigal, 2012), and the invasion of this anthropogenic CO_2 into the coastal ocean may increase seagrass production (Zimmerman et al., 2015). Hu and Cai (2013) demonstrated that acidification (due to anthropogenic CO_2 emissions and eutrophication) was greater for estuaries receiving lower loads of HCO_3^- and other weathering products from their respective rivers. A subsequent analysis reinforced this concept by showing that a majority of Texas estuaries are experiencing long-term acidification, driven largely by reduced alkalinity loads stemming from drought and human water use (Hu et al., 2015). The potential for acidification in estuaries not experiencing drought has received less attention, despite the fact that acidification may have particularly severe impacts on the economies of communities surrounding these estuaries (Ekstrom et al., 2015). Recent studies have indicated that estuaries receiving moderate or low alkalinity loads from their tributary rivers (like those of eastern North Carolina) may be particularly vulnerable to acidification due to mixing with ocean waters high in dissolved CO_2, as well as those receiving inputs of acidity through aerobic (Hu & Cai, 2013) and anaerobic pathways (Cai et al., 2017). Therefore, knowledge of how carbonate buffering varies between estuaries experiencing the same climatic conditions but different riverine end-member chemistries is critical if we are to predict how coastal systems will respond to future acidification.

Climate change is expected to alter current hydrologic patterns, and these changes will affect estuarine carbon (C) cycling on seasonal to decadal scales (Dhillon & Inamdar, 2013; Najjar et al., 2010). In addition to these longer-term effects, episodic events like storms and droughts are also expected to increase with climate change and will contribute significantly to estuarine CO_2 fluxes on an annual scale, although the nature of that change will depend on a variety of system-specific features (Crosswell et al., 2012; Evanset al., 2013; Hunt et al., 2013; Ruiz-Halpern et al., 2015). Both episodic and seasonal variations in river discharge strongly affect air-water CO_2 exchange in estuaries (Bauer et al., 2013; Borges & Abril, 2012; Cai, 2011; Chen et al., 2013); however, quantitative relationships between estuarine C cycling and catchment hydrology remain relatively poorly defined.

2. Materials and Methods

2.1. Study Site

The Neuse River flows from the urbanized North Carolina Piedmont in the Raleigh-Durham-Chapel Hill Triangle area through the coastal plain, toward its terminus in Pamlico Sound, the third largest estuarine

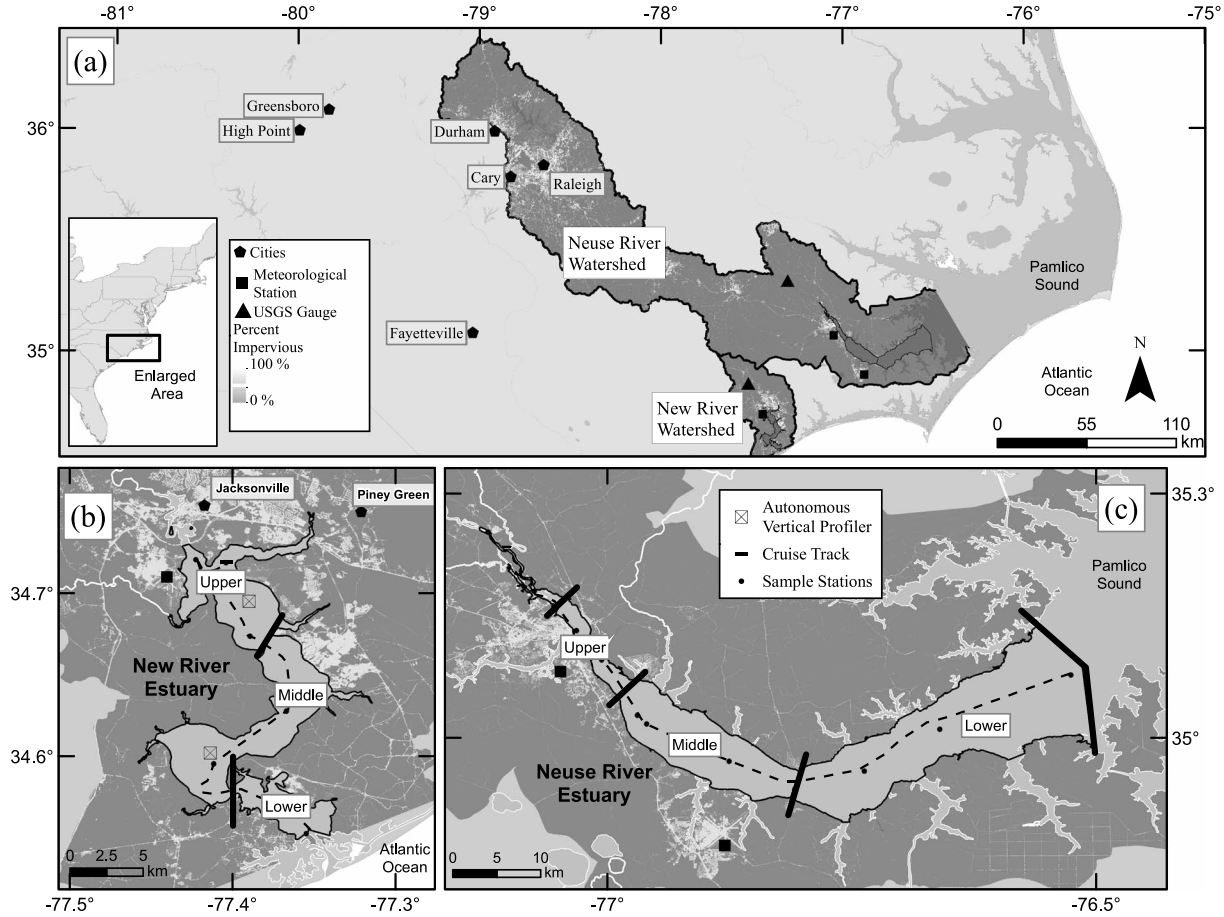

Figure 1. (a) General site map showing the locations of the NewRE and NeuseRE, their respective watersheds (dark gray), and USGS stream flow gauges (black triangles) for which river discharge measurements were obtained. Detailed maps of the (b) NewRE and (c) NeuseRE showing the location of meteorological stations (black squares), autonomous vertical profilers (AVPs, hollow squares), discrete sampling stations (black circles), and dataflow cruise track (dashed line).

system in North America (~7,770 km^2; Figure 1). The Neuse River Estuary (NeuseRE) begins near New Bern, NC, where the funnel-shaped estuary widens considerably and oligohaline conditions prevail. Due to restricted exchange across the narrow inlets of Pamlico Sound, astronomical tides are minimal (<10 cm); lateral and longitudinal water movements are mostly driven by meteorological factors like wind and freshwater discharge (Luettich et al., 2000); hence, we consider this estuary to be "river-dominated." Submarine groundwater discharge to the estuary is small relative to inputs of water and nutrients from the Neuse and Trent rivers (Fear et al., 2007; Null et al., 2011). This system has been well studied for decades via long-term monitoring projects like the Neuse River Estuary Modeling and Monitoring program (ModMon; http://www.unc.edu/ims/neuse/modmon/). A history of accelerated anthropogenic nutrient loading, largely related to agricultural and urban development, has driven eutrophication in this system since the 1970s, with primary productivity estimated at between 200 and 500 g C m^{-2} yr^{-1} (Boyer et al., 1993; Mallin et al., 1993). A combination of these factors leads to frequent phytoplankton blooms and bottom water hypoxia (Paerl et al., 1998, 2007).

The New River is a small coastal plain river, located entirely in Onslow County, NC, USA. Agricultural land use dominates its watershed, which is approximately one tenth the size of the Neuse River watershed. The upper estuary is surrounded by the city of Jacksonville, NC, with a 2010 census population of over 70,000 (Figure 1). Impervious surfaces, along with the small size of the watershed, cause river inputs to the New River Estuary (NewRE) to be relatively "flashy," with discharge quickly peaking and receding after storms (Peierls et al., 2012). Because of relatively low river discharge and long residence time, we consider this estuary to exemplify "marine-dominated" traits. Before transitioning into the oligohaline NewRE near Jacksonville, NC, the

New River enters a relatively short (~12 km) tidal freshwater reach, where N loads are attenuated by denitrification in the surrounding forested wetlands (Ensign et al., 2013; Von Korff et al., 2014). The body of the NewRE consists of five interconnected lagoons of differing sizes. The seaward lagoon is connected to the Atlantic Ocean by a narrow inlet that limits oceanic exchange. The tidal amplitude is correspondingly low, ranging from approximately 0.25 m in middle and upper segments to nearly 1 m at the New River Inlet. This low tidal amplitude, along with freshwater discharge, drives vertical stratification and frequent bottom water hypoxia, as often occurs in the NeuseRE. Following upgrades to a sewage treatment plant in 1998, primary production in the NewRE decreased, causing a transition from eutrophic (250–500 g C m^{-2} yr^{-1}) to mesotrophic status (<250 g C m^{-2} yr^{-1}) (I. C. A. Anderson, personal communication, 2015; Mallin et al., 2005). Fringing marshes are present in both estuaries but constitute a relatively small fraction of the intertidal area; salt marshes and swamps represent approximately 21 and 6% of the shoreline in the NewRE (Currin et al., 2015).

2.2. Synoptic Surveys

From October 2014 to October 2016, 74 high-resolution surveys of surface water partial pressure CO_2 (pCO_2) were conducted at biweekly to monthly intervals, 36 in the NeuseRE and 38 in the NewRE. Twenty-one of the NewRE surveys were conducted as part of a study investigating diel pCO_2 variability, during which three consecutive surveys were completed in a contiguous 25 h period, at dawn of the first day, dusk of the first day, and dawn of the following day. For the purposes of general comparisons in this study, these dawn-dusk-dawn surveys were combined into seven representative daily averages. All other surveys began in the midmorning (08:30–10:00 AM). The choice of a midmorning sampling time may lead to a small overestimation of pCO_2 due to diurnal variations but has been used extensively because it is close to the idealized midpoint between dawn pCO_2 maxima and dusk pCO_2 minima (Crosswell et al., 2012; Maher & Eyre, 2012). For the purpose of this interestuary comparison, CO_2 fluxes were estimated from longitudinal transects alone, which covered slightly different regions of each estuary. Because of the small size of the NewRE, a wide salinity range (~5–35) was surveyed during each transect. The surface area of the NeuseRE is ~4 times greater than the NewRE; thus, fixed stations covered a smaller section of the salinity range in this system (0 to ~20). The NeuseRE becomes strongly influenced by other watersheds (i.e., Tar-Pamlico) beyond the downstream extent of the lowest estuarine segment (Figure 1).

2.3. CO_2 Flux Determinations

Both estuaries were divided into three morphologically distinct sections along their respective longitudinal axes (Figure 1), such that each estuary's mouth is the point at which other watersheds become influential. These divisions are consistent with previous studies in the NeuseRE (Crosswell et al., 2012) and NewRE (Crosswell et al., 2017). In situ pCO_2 was measured using a combined laminar flow showerhead equilibrator and infrared detector (LI-COR, Li-840A). Analyzers of this type have been deployed extensively in previous studies (Crosswell et al., 2012, 2014, 2017; Frankignoulle & Borges, 2002; Santos, Maher, & Eyre, 2012; Wang & Cai, 2004; Zhai et al., 2005). Water was continuously pumped from a depth of approximately 0.5 m (variable with boat speed) into a showerhead equilibrator, and air was circulated between this equilibrator and the infrared analyzer. Water was also sent through a flow-through cell (Dataflow) for measurements of chlorophyll *a* fluorescence (chl *a*), dissolved oxygen (DO), pH, salinity, temperature, and turbidity (YSI 6600 multiparameter sonde, Yellow Springs Inc, Yellow Springs, OH). Measurements were recorded at 0.5 Hz, corresponding to a spatial resolution of ~6 m at a boat speed of ~40 km h^{-1}. The raw CO_2 mixing ratio in the equilibrator (xCO_2) was calibrated against two to three standards, ranging from 100 to 5,000 ppm (certified to ±2%), before and after each cruise, when measurements of atmospheric pCO_2 ($pCO_{2(air)}$) were also made. This calibration curve was extrapolated linearly for xCO_2 beyond 5,000 μatm. $pCO_{2(water)}$ was calculated from calibrated xCO_2 in the equilibrator according to equation (1), where T_w and T_{SHE} are measured temperatures in the water and equilibrator, respectively.

$$pCO_{2(water)} = xCO_2 \times e^{(0.0423 \times [T_w - T_{SHE}])} \quad (1)$$

Average pCO_2 was calculated for each segment, weighting each measurement by the distance between sampling points (shipboard GPS) and the surface area of each segment. Daily average pCO_2 was then estimated by applying a linear interpolation to segment-average pCO_2 from individual cruise dates. These interpolated

segment-average pCO_2 estimates were then used to calculate CO_2 flux (mmol C cm^{-2} h^{-1}) using the stagnant-layer model (Smethie et al., 1985) according to equation (2):

$$\text{flux} = k \times K_o \times \Delta pCO_2 \tag{2}$$

where ΔpCO_2 is the air-water pCO_2 gradient. By convention, a positive ΔpCO_2 indicates $pCO_{2(water)}$ greater than $pCO_{2(air)}$. K_o is the CO_2 solubility coefficient (Weiss, 1974). The gas transfer velocity, k (cm h^{-1}) was calculated using the following equation from Jiang et al. (2008):

$$k = \left[\left(0.314 \times U_{10}{}^2 - 0.436 \times U_{10} + 3.99\right) \times \left(Sc_{SST}/600\right)\right]^{-0.5} \tag{3}$$

where U_{10} (m s^{-1}) is the daily averaged wind speed normalized to a height of 10 m. A brief discussion of the limitations of this method, including a sensitivity analysis of CO_2 flux using different k parameterizations, is included in the supporting information (Figure S2). Briefly, the use of different k parameterizations may overestimate or underestimate CO_2 flux by a factor of ~1.6–2 (Table S1). However, we chose the parameterization of Jiang et al. (2008) because it constitutes an intermediate estimate of k, considers both marine- and river-dominated estuaries, and is consistent with previous studies in both the NeuseRE (Crosswell et al., 2012) and NewRE (Crosswell et al., 2017). Hourly average wind speed was obtained from two autonomous vertical profilers deployed in the NewRE (Reynolds-Fleming et al., 2002), and from two meteorological stations (KEWN and KNKT) near the NeuseRE (Figure 1). Sc_{SST} is the Schmidt number for CO_2 at ambient sea surface temperature (SST) and sea-surface salinity (SSS). Because sampling began near the middle of 2014, study years rather than calendar years were used to calculate annual fluxes (Year 1: 27 October 2014 to 26 October 2015; Year 2: 27 October 2015 to 16 October 2016).

Discrete samples for dissolved inorganic carbon (DIC) measurements were collected by a diaphragm pump at the surface and ~0.5 m from the bottom, stored in a refrigerator unpreserved with no headspace in 20 mL scintillation vials, and analyzed on a Shimadzu TOC-5000A within 24 h. Previous studies have shown a difference between DIC in preserved and unpreserved samples (Crosswell et al., 2012); however, this difference is small relative to observed spatial and temporal variability in DIC. Hence, no correction was applied to DIC values here. CO2sys (Lewis & Wallace, 1998) was used to calculate all additional carbonate system parameters, including total alkalinity (TA) and Revelle factor (R). Carbonic acid dissociation constants (K_1 and K_2) of Dickson and Millero (1987) were assumed, and the National Bureau of Standards scale was used for pH. Measured pCO_2, DIC, SST, and SSS were used as CO2sys inputs. pCO_2 measurements were only used when the boat was stationary for a sufficient time (at least 10 min) to ensure system equilibration with the parcel of water being sampled for DIC, temperature, and salinity.

Nonlinear changes in pCO_2 occur when mixing or net biological processes alter the concentration of DIC, and these changes are buffered to an extent that is determined by the relative concentrations of TA and DIC. Because both TA and DIC vary across the estuary, this carbonate buffering also exhibits spatial and temporal variability. Previous studies have shown the presence of a minimum buffering zone (MBZ) in mesohaline portions of some tropical and subtropical estuaries (Hu & Cai, 2013; Jeffrey et al., 2016; Ruiz-Halpern et al., 2015). At this MBZ, when temperature and salinity are held constant, pCO_2 is most sensitive to additional inputs of DIC. Here pH is approximately halfway between the pK_1 and pK_2 of H_2CO_3 (Cai et al., 2011), the ratio of DIC:TA approaches unity, and the Revelle factor is maximized. The Revelle factor (R) is a commonly used buffer factor of the carbonate system, defined as $\partial \ln(pCO_2)/\partial \ln(\text{DIC})$, and is implicitly related to the ratio of DIC:TA (Egleston et al., 2010). In this study, we calculate R in CO2sys (Lewis & Wallace, 1998) using paired measurements of DIC, pCO_2, T, and S. While the carbonate system can be quantitatively assessed using other sets of paired observations (DIC and TA, pCO_2 and pH, etc.), the combination of DIC and pCO_2 is preferred, given the current uncertainty in carbonate system measurements (Millero, 2013). We assess spatial and temporal variations in R and discuss them in the context of riverine TA and DIC inputs and ocean acidification.

2.4. Freshwater Age

A variety of metrics are used to assess the flow of C (and other properties) through ecological systems and the time scales involved, known as "system diagnostic times" (Sierra et al., 2017). In estuaries, terms like residence time, transit time, and age are often used, but their calculation often requires assumptions of steady state or homogeneous mixing, which are often not met (Alber & Sheldon, 1999). A lag time exists for water flowing between the head and mouth of all estuaries, meaning that the time for a given particle to exit the system

varies along its length. Additionally, river flow can change rapidly, and if water residence time is to be calculated as the ratio of estuarine volume to river discharge, then the averaging time interval for discharge must be appropriate.

In this study, freshwater age (FW age) was calculated for each sampling date and for each segment using calculated freshwater volume and river discharge, obtained for the New River near Gum Branch (USGS gage #02093000), and for the Neuse River near Ft Barnwell (USGS #02091814). Given the location of these gauges far upstream of the estuary, and the presence of tributaries between the gauge and the estuary, it was necessary to scale discharge by dividing it by the ratio of total to gauged watershed (0.22 and 0.69 for the NewRE and NeuseRE, respectively) (Ensign, Halls, & Mallin, 2004; Peierls et al., 2012). The time period over which river discharge was averaged was then calculated using the "date-specific" method of Alber and Sheldon (1999) (Peierls et al., 2012). This method provides a robust estimate of the amount of time needed for river discharge to replace the volume of freshwater in the estuary. FW age for each estuarine segment was calculated as a cumulative sum, including all upstream segments.

2.5. Estuarine Versus Riverine Contributions to CO_2

Allochthonous, river-borne CO_2 is released to the atmosphere in estuaries, but it is also replenished when riverine organic carbon (OC) is respired to CO_2 in estuaries. The balance between these autochthonous and allochthonous contributions to CO_2 degassing is difficult to discern and likely varies in estuaries ranging from river-dominated, like the NeuseRE, to marine-dominated systems like the NewRE. We estimated the relative contributions of river-borne and estuarine CO_2 sources ($[CO_2]_{river}$ and $[CO_2]_{estuary}$) for both the river-dominated NeuseRE and the marine-dominated NewRE using methods adapted from Jiang et al. (2008) and Joesoef et al. (2015). In essence, CO_2 delivered by the river was balanced against losses due to air-water exchange (integrated over the cumulative FW age), with the remainder attributed to net estuarine production.

First, for each segment and sampling date, the contribution of DIC due to mixing with ocean water ($DIC_{mixing\ w/O}$) was calculated using equation (4):

$$DIC_{mixing\ w/O} = DIC_{ocean} \times S_i / S_{ocean}, \tag{4}$$

where S_i and S_{ocean} are the average salinities for each estuarine segment and the ocean (35), respectively, while DIC_{ocean} is the DIC concentration of the oceanic end-member (2,000 μmol kg^{-1}). The remaining DIC was attributed to mixing with river water ($DIC_{mixing\ w/R}$):

$$DIC_{mixing\ w/R} = DIC_{mixing\ w/O} + DIC_{river} \times (1 - S_i / S_{ocean}), \tag{5}$$

where DIC_{river} is the measured or modeled DIC concentration of river water for that date. DIC_{river} in the NewRE was estimated as the 0 salinity end-member for each date using a linear regression of measured estuarine DIC and salinity. An implied assumption of linear mixing may add a small uncertainty to subsequent calculations. DIC_{river} in the Neuse was measured, so it was not necessary to model this value. Both of these calculations were repeated for TA (oceanic end-member was assumed to be 2,200 μmol kg^{-1}), allowing CO_2 contributions from mixing with both river water and the ocean ($[CO_2]_{mixing\ w/R}$ and $[CO_2]_{mixing\ w/O}$, respectively) to be calculated with DIC, TA, and a *T*- and *S*-dependent equation of solubility (Weiss, 1974). The direct CO_2 contribution from riverine DIC and TA loading ($[CO_2]_{river}$) was then calculated as

$$[CO_2]_{river} = [CO_2]_{mixing\ w/R} - [CO_2]_{mixing\ w/O}. \tag{6}$$

The concentration of CO_2 produced within the estuary ($[CO_2]_{estuary}$) was then assumed to be equivalent to the difference between the measured $[CO_2]$ and $[CO_2]_{mixing\ w/R}$, accounting for losses due to air-water CO_2 exchange, according to equation (7):

$$[CO_2]_{estuary} = [CO_2]_i - [CO_2]_{mixing\ w/R} + (\tau_i \times F_i). \tag{7}$$

Here $(\tau_i \times F_i)$ is the temporally integrated CO_2 flux for each segment, where τ_i is the freshwater age, as calculated using the methods presented in Alber and Sheldon (1999), and F_i is the segment-average CO_2 flux. $[CO_2]_i$ is the segment-wide average of measured CO_2 concentration, adjusted for solubility at measured temperature and salinity (Weiss, 1974).

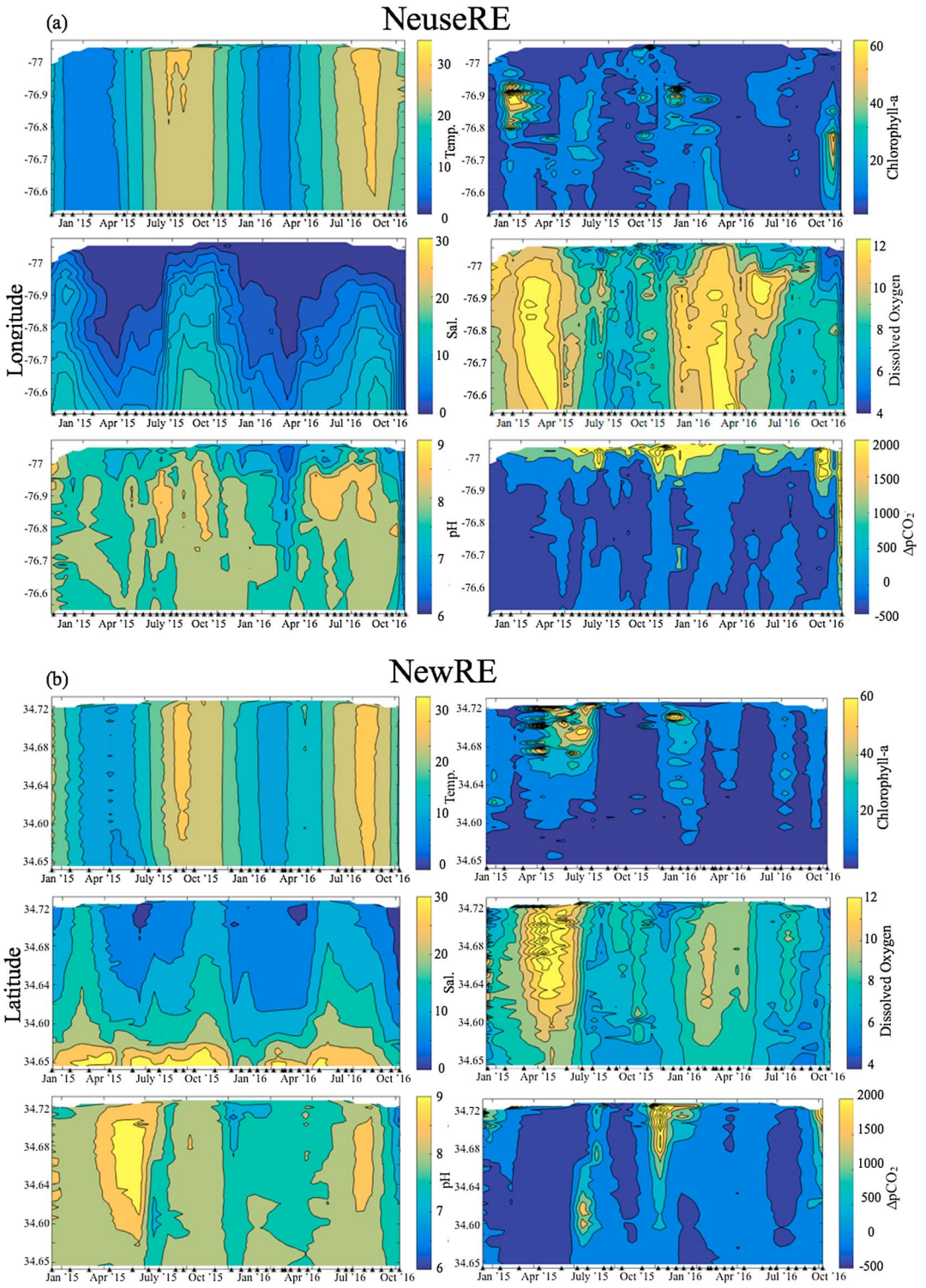

Figure 2. Contour plots showing longitudinal transects (vertical axis) through time (horizontal axis) for both the (a) NeuseRE and (b) NewRE constructed using a linear interpolation method. The approximate timing of pCO_2 surveys are indicated as the black triangles along the horizontal axis. Because the longitudinal axis of the NewRE is oriented in the north-south direction, latitude (decimal degrees) is used to represent distance down this estuary. Distance along the east-west oriented NeuseRE is represented with longitude (decimal degrees). Temperature (°C), salinity, pH, chlorophyll *a* ($\mu g\ L^{-1}$), dissolved oxygen ($mg\ L^{-1}$), and ΔpCO_2 (μatm) are shown as the respective color axes.

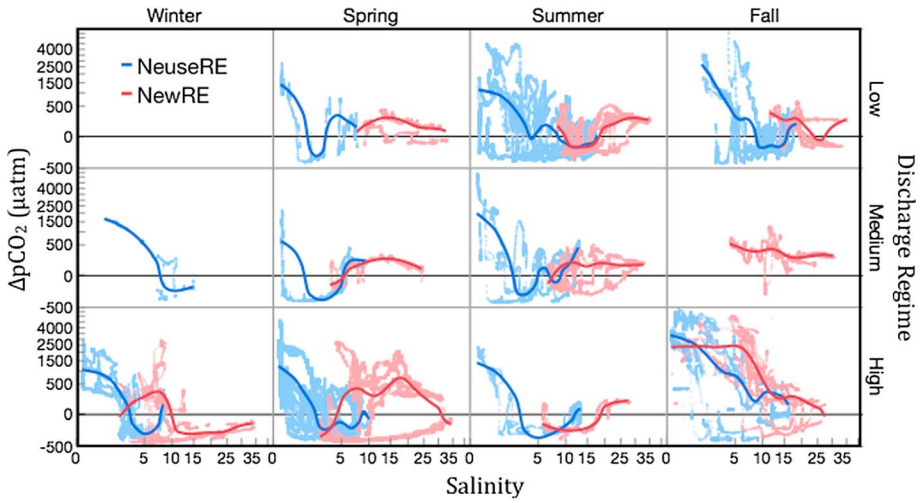

Figure 3. Seasonal relationship between salinity and ΔpCO_2 (μatm), shown for low-, medium-, and high-discharge conditions in the NewRE (red) and NeuseRE (blue). Discharge regimes were determined as the first quartile, median, and second quartile of daily average discharge statistics from 2007 to 2017. The black line at $\Delta pCO_2 = 0$ indicates air-water pCO_2 equilibrium, while the blue and red lines show smoothing spline fits for the NeuseRE and NewRE, respectively.

3. Results

3.1. Physicochemical and Biological Setting

Segment-average salinity ranged from <5 to 34 in the NewRE but never exceeded 17 in the NeuseRE (Figures 2a and 2b). Seasonal trends, however, were very similar. High salinity in summer gave way to fresher conditions during the winter and spring, when precipitation in the watershed exceeded evapotranspiration (Litaker et al., 2002; Paerl et al., 2014). In the winter of 2015, maximum salinity in the NeuseRE was below the minimum salinity in the NewRE. Chlorophyll *a* (in situ fluorescence) was generally low (< 10 μg L^{-1}), but episodic phytoplankton blooms were associated with elevated chlorophyll *a* (up to 150 μg L^{-1}) in the late fall/early winter of both 2014 and 2015. Blooms were often restricted to the upper or middle region of the estuary where they contributed to elevated DO and pH as high as 9.4 and 10.7 (midday sampling) in the NewRE and NeuseRE, respectively.

3.2. Spatial pCO_2 Trends

In general, pCO_2 decreased from the river toward the ocean, a trend that was most pronounced in the NeuseRE, where air water pCO_2 gradients (ΔpCO_2) often transitioned from positive to negative along the estuarine salinity gradient (Figure 2). Rapid increases in ΔpCO_2 below a salinity of 5 occurred irrespective of season or discharge condition in the NeuseRE (Figure 3). This trend is less evident in the NewRE, occurring nearly exclusively in the fall during high discharge conditions. The highest measured ΔpCO_2 values occurred in the upper estuary, with segment-average ΔpCO_2 reaching 4,654 (range = 3,310–5,806 μatm) and 3,480 μatm (range = 3,303–5,112 μatm) in the upper NeuseRE (September 2016) and NewRE (October 2015), respectively. These large pCO_2 supersaturation events corresponded with the lowest segment-average DO in both the NewRE (5.56 mg L^{-1}) and the NeuseRE (5.56 mg L^{-1}). Extreme CO_2 undersaturation was observed during the phytoplankton bloom in the winter/spring of 2015, with lowest segment-average pCO_2 of 99 in the middle NewRE, corresponding with relatively high DO (10.63 mg L^{-1}). The lowest pCO_2 was in the spring of 2016, at 72 μatm in the middle NeuseRE, also corresponding with elevated DO (11.69 mg L^{-1}).

While Figure 3 shows that ΔpCO_2 and salinity were generally negatively related, there was a high degree of variability in the relationship. Instances of positive and negative ΔpCO_2 can be found during all seasons and all discharge regimes, across the estuarine salinity range. However, a general trend of high pCO_2 across the salinity gradient during the fall transitioning to low pCO_2 conditions during the winter and spring can be observed. The highly variable relationship between ΔpCO_2 and salinity (Figure 3), as well as the "patchy"

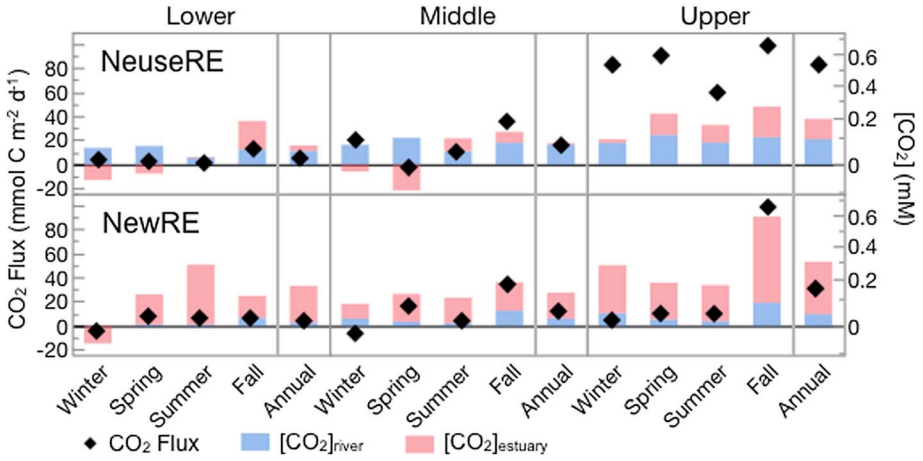

Figure 4. Estuarine (red bar) and river-borne (blue) CO_2 sources (mM), as well as CO_2 flux (black diamond) by season and section for the (top) NeuseRE and (bottom) NewRE.

nature of pCO_2 distributions on any given date (Figure 2), suggests that biological production and consumption are important drivers of pCO_2 in these shallow estuaries. The observed covariation in CO_2 and DO, occurring across all estuarine segments (Figure 2), supports the idea that regional variations in biological activity (photosynthesis and respiration) drive CO_2 distributions, irrespective of location along the salinity gradient.

3.3. Air-Water CO_2 Flux

System averaged ΔpCO_2 in both the NewRE and NeuseRE was generally positive (Figure 2); thus, both estuaries were most often sources of CO_2 to the atmosphere. Two major degassing events were seen in the fall of 2015 and 2016, both associated with the impact of large tropical weather systems, Hurricanes Joaquin and Matthew, respectively. Despite most of the estuarine surface area being at or near saturation with respect to the atmosphere (Figure 2), high pCO_2 in the upper segments generally maintained a positive air-water CO_2 exchange, particularly when river discharge was high, during the fall months (Figures 3 and S4). Between years 1 and 2, annual average CO_2 flux increased from 15.7 to 16.9 mmol C m^{-2} d^{-1} in the NewRE (an 8% increase) and from 7.7 to 17.5 mmol C m^{-2} d^{-1} (127% increase) in the NeuseRE. These enhanced CO_2 fluxes coincided with 27 and 32% increases in river discharge from year 1 to year 2 for the Neuse and New Rivers, respectively (Table 2). Over the 2 year study period, discharge was 180% of the antecedent 10 year average for the NewRE, 153% for the NeuseRE.

3.4. Freshwater Age

During the 2 year study period, FW age ranged from 6.9 to 136 days in the NeuseRE ($\bar{x} = 58$), and from 9.1 to 91 days in the NewRE ($\bar{x} = 46$) (Figure S3). Generally, FW age was low in the winter ($\bar{x} = 29$ and 27 days in the NewRE and NeuseRE, respectively) and increased through the spring to a summer maximum of ~3 months ($\bar{x} = 71$ and 84 days in the NewRE and NeuseRE, respectively). Storm events in the middle to late fall resulted in the lowest calculated FW ages. Minimum FW ages were observed at the end of the study, when 15–46 cm of rain fell on eastern NC during Hurricane Matthew, causing FW age to drop as low as 7 to 9 days. Between

Table 1
Site Description and Average Physical and Chemical Properties

Estuary	Type	Surface area (km^2)	Water depth (m)	Watershed area (km^2)	FW age (days)	Total alkalinity ($\mu mol\ kg^{-1}$)	DIC ($\mu mol\ kg^{-1}$)
New	Marine-dominated, lagoonal	78.7	1.8	1,024	46 (±26.9)	River: 945 (±275) Estuary: 1,302 (±444)	River: 1,034 (±237) Estuary: 1,298 (±366)
Neuse	River-dominated, lagoonal	352.1	2.7	15,700	58 (±33.6)	River: 349 (±172) Estuary: 860 (±442)	River: 456 (±177) Estuary: 817 (±371)

Note. Standard deviations are shown in parentheses.

Table 2
Air-Water CO_2 Flux as Seasonal and Annual Averages (mmol C m^{-2} d^{-1})

	New River Estuary				Neuse River Estuary			
	Upper	Middle	Lower	Total	Upper	Middle	Lower	Total
Surface area (km^2)	28	38	12	79	22	100	230	352
Average salinity (±SD)	10.6 (4.5)	15.6 (4.2)	26.7 (3.7)	15.5	1.2 (1.6)	4.2 (3.1)	8.2 (4.1)	6.6
Winter	4.4	−6.6	−4.6	−2.37	82.6 (100)	20.1 (37.9)	3.7 (−22.0)	13.3 (2.6)
Spring	9.9	16.2	7.7	12.6	90.2 (29.1)	−2.7 (−2.4)	2.3 (2.8)	6.35 (2.96)
Summer	9.8	3.9	6.2	6.5	59.6 (22.3)	10.2 (−3.8)	0.9 (−0.5)	7.2 (−0.02)
Fall	98.4	34.1	6.2	52.7	98.4 (115)	35.5 (55.3)	12.7 (13.9)	24.5 (31.96)
Year 1	25.2	12.1	5.5	15.7	77.9	8.2	0.7	7.7
Year 2	32.2	10.4	2.4	16.9	86.7	22.6	8.8	17.5
Total	28.6	11.3	4.0	16.3	82.2 (66.6)	15.3 (21.8)	4.7 (−1.4)	12.5 (9.38)

Note. Values in parenthesis are previous estimates from the NeuseRE (Crosswell et al., 2012) or standard deviations of segment-average salinity.

years 1 and 2, annual average FW age decreased from 66 to 54 days in the NeuseRE and from 47 to 45 days in the NewRE, consistent with increases in freshwater discharge.

3.5. Riverine Versus Autochthonous CO_2

Riverine CO_2 inputs ($[CO_2]_{river}$) were greater in the river-dominated NeuseRE than in the marine-dominated NewRE, by a factor of 2.6, 3.4, and 5.2 for the upper, middle, and lower segments, respectively (Figure 4). Seasonally, $[CO_2]_{river}$ was low in the summer and greatest during the spring and fall, when river discharge and ΔpCO_2 were high (Figure 3). For systems with similar watershed characteristics and climatology, $[CO_2]_{river}$ should scale with the ratio of watershed: estuary surface area. This ratio is 4 times greater for the NeuseRE than for the NewRE (Table 1), offering a partial explanation for the consistently larger $[CO_2]_{river}$ in the NeuseRE. $[CO_2]_{river}$ was above 0 along the length of both estuaries and decreased toward the ocean. As with $[CO_2]_{river}$, $[CO_2]_{estuary}$ was greatest in the upper segments and quickly decreased toward the ocean, analogous to the negative relationship between pCO_2 and FW age (Figure 7). $[CO_2]_{estuary}$ was larger in the NewRE than in the NeuseRE by a factor of 3, 18, and 7 for the upper, middle, and lower segments, respectively (Figure 4). This suggests that internal sources of CO_2 (i.e., respiration) to surface waters were more important in the NewRE, despite both estuaries releasing a similar amount of CO_2 to the atmosphere (Table 2). That pCO_2 appears to increase more at lower salinity in the NeuseRE (Figure 3) supports the notion that riverine sources of CO_2 play a larger role in the river-dominated NeuseRE than in the marine-dominated NewRE. Seasonally, $[CO_2]_{estuary}$ was greatest in the fall, most notably in the upper regions of both estuaries, and was lowest during the winter and spring, coinciding with elevated chl *a* and DO, and relatively low temperature (Figure 2). To further investigate the relative importance of riverine and estuarine processes on CO_2 dynamics in these systems, segment-average CO_2 flux was regressed on both $[CO_2]_{river}$ and $[CO_2]_{estuary}$ (Figure 6).

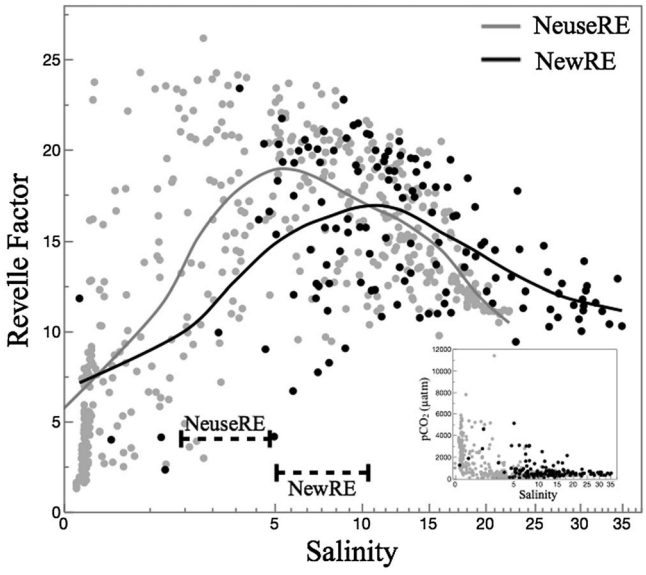

Figure 5. Scatterplot of Revelle factor against salinity for the NeuseRE (gray line) and NewRE (black line). Approximate locations of the minimum buffer zones (MBZs) are bounded near the bottom of the figure. Line is a smoothing spline fit ($\lambda = 0.2$). An inset of pCO_2 and salinity is included, showing that the region of greatest CO_2 oversaturation occurs at a lower salinity in the NeuseRE than in the NewRE.

3.6. Buffering Effects

As in previous studies (Hu & Cai, 2013; Ruiz-Halpern et al., 2015), *R* was very low in the oligohaline portion of the NewRE and NeuseRE, and increased rapidly with salinity to a midestuary maximum (Figure 5). At this point, *R* decreased as low alkalinity river water mixed with seawater with a DIC:TA ratio less than 1. The MBZ, where *R* is maximized and water is poorly buffered, occurred at a lower salinity in NeuseRE (2–5) than in NewRE (5–10), coinciding with the upper NewRE and upper/middle segments of the NeuseRE, both of which constitute ~35% of the surface area of each estuary (Table 2).

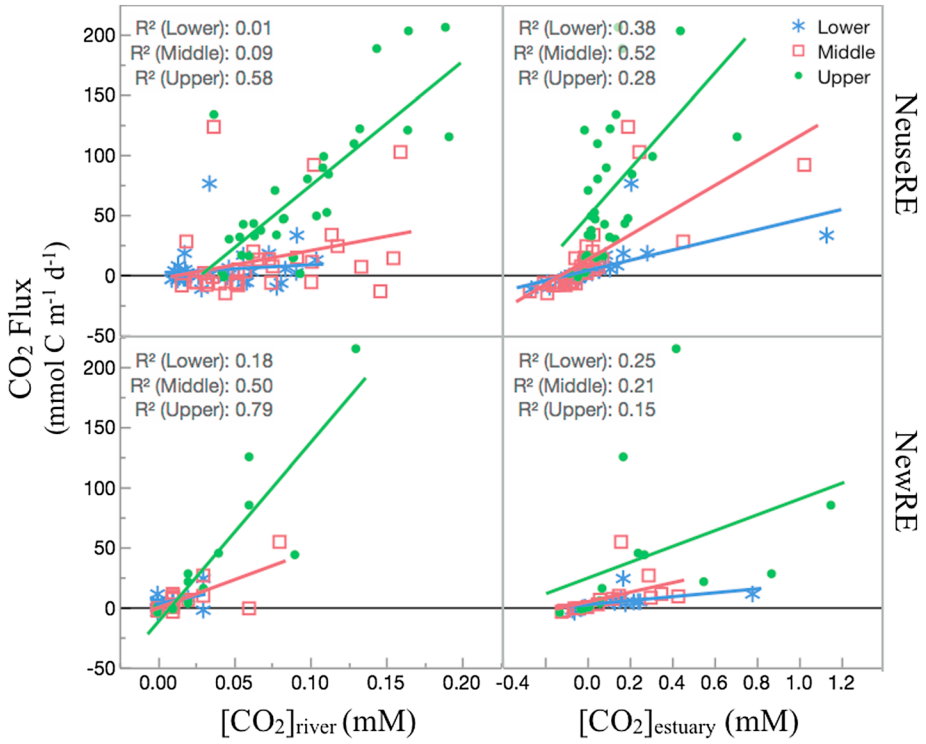

Figure 6. Linear regressions between river-borne ($[CO_2]_{river}$), estuarine CO_2 ($[CO_2]_{estuary}$), and air-water CO_2 flux (mmol C m^{-2} d^{-1}). CO_2 flux was most strongly correlated with $[CO_2]_{river}$ in upper estuarine segments (R^2 = 0.58 to 0.79) but with $[CO_2]_{estuary}$ in middle and lower segments (R^2 = 0.21 to 0.52).

4. Discussion

4.1. Air-Water CO_2 Flux

Globally, estuaries release approximately 20–40 mmol C m^{-2} d^{-1} to the atmosphere (Laruelle et al., 2013; Maher & Eyre, 2012; Regnier et al., 2013). We estimate CO_2 effluxes in the NewRE and NeuseRE to be well below this average, between 15.7 and 16.9 mmol C m^{-2} d^{-1} and between 7.7 and 17.5 mmol C m^{-2} d^{-1}, respectively. Despite differences in morphology and surrounding land use between these estuaries (Table 1), annual CO_2 fluxes were quite similar (Table 2). However, CO_2 fluxes in the NeuseRE were ~30% greater than previously reported, demonstrating the effect of interannual-scale hydrologic variability on pCO_2 and associated fluxes. This large interannual variability in CO_2 flux, relative to between-estuary variability, indicates that data collected over a single year may not represent the long-term average. Hence, the nature of this hydrologic forcing must be better understood before CO_2 fluxes from these microtidal, lagoonal estuaries can be scaled globally and over longer time periods.

To further investigate the relative importance of riverine and estuarine processes on CO_2 dynamics in these systems, segment-average CO_2 flux was regressed on both $[CO_2]_{river}$ and $[CO_2]_{estuary}$ (Figure 6). In all cases, the correlation coefficient (R^2) between $[CO_2]_{river}$ and CO_2 flux decreases from the upper to lower segments, highlighting the importance of river-borne CO_2 on outgassing in the upper segments of both estuaries. $[CO_2]_{estuary}$ was also correlated with CO_2 flux, with highest R^2 values in the middle and lower segments. Taken together, these results suggest that in river-dominated microtidal estuaries like the NeuseRE, biological processing drives the trend of decreasing pCO_2 from the head of the estuary to the mouth, while riverine CO_2 inputs have a larger impact on the magnitude of total estuarine CO_2 flux. In marine-dominated estuaries like the NewRE, however, internal production of CO_2, rather than riverine inputs appear to drive CO_2 oversaturation. While submarine groundwater discharge may be a significant DIC source in some estuaries (Call et al., 2015; Macklin et al., 2014; Santos et al., 2010), this source has been determined to be small in both the NeuseRE (Fear et al., 2007; Null et al., 2011) and NewRE (Crosswell et al., 2017). Previous studies have identified river-dominated estuaries as large CO_2 sources, relative to marine-dominated ones (Akhand et al., 2016; Jiang

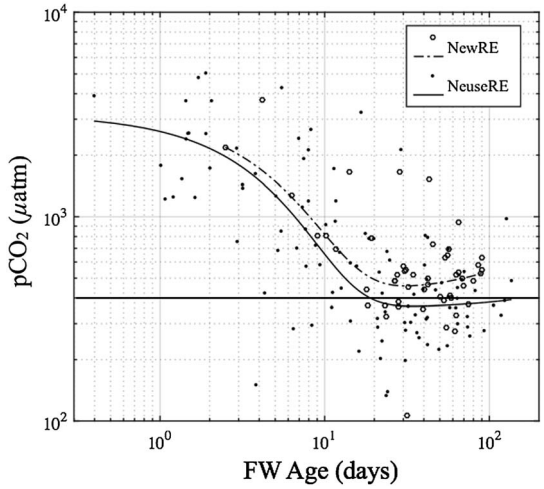

Figure 7. FW age (days) versus pCO_2 (μatm), with exponential fits of the form: $f(x) = a \times e^{(b \times x)} + c \times e^{(d \times x)}$. $R^2 = 0.857$ for the NeuseRE and $R^2 = 0.861$ for the NewRE. The horizontal line represents pCO_2 equilibrium with the atmosphere (~400 μatm).

et al., 2008). Our findings support this understanding; we show that river-borne CO_2 ($[CO_2]_{river}$) was indeed larger in the river-dominated NeuseRE than in the marine-dominated NewRE, by a factor of 2.6–5.2. However, CO_2 generated within the estuary ($[CO_2]_{estuary}$) was greater in the NewRE by a factor of 3–18, causing annual CO_2 fluxes to be similar between estuaries.

4.2. Freshwater Age

As shown in Figure 7, pCO_2 is maximized when FW age is short, consistent with trends observed for small lakes (Vachon & del Giorgio, 2014), global inland waters (Catalán et al., 2016; Hotchkiss et al., 2015), and modeled estuaries along the U.S. East Coast (Laruelle et al., 2017). Coincidentally, highest CO_2 fluxes were observed in response to Hurricanes Joaquin (late September 2015) and Matthew (early October 2016), when both estuaries were rapidly flushed. That $[CO_2]_{estuary}$ was greatest during the fall in both estuaries (Figure 4) indicates that net ecosystem respiration of riverine organic matter (OM), rather than riverine CO_2 inputs, is responsible for much of the CO_2 released during this period. While bioassays in the NewRE indicate that only ~20% of riverine DOC is labile (I. Anderson, personal communication, 2016), the respiration of this DOC alone is sufficient to sustain the increased pCO_2 we observe (Figure 3). For example, respiration of 20% of the average riverine DOC (600 μM) would generate 120 μM DIC, causing pCO_2 to increase by nearly 80%, from 4,437 μatm to 7,961 μatm (depending on TA). CO_2 inputs of this magnitude are sufficient to account for the large and nonlinear increases in pCO_2 observed at low salinity (Figure 3). Additionally, the respiratory DIC inputs assumed here (120 μM) are of similar order to $[CO_2]_{estuary}$ in the upper regions of both estuaries (Figure 4), further supporting the autochthonous nature of this CO_2 source.

As FW age increases, reductions in $[CO_2]_{estuary}$ cause pCO_2 to approach equilibrium with the atmosphere, reaching a minimum at around 14–30 days (Figure 7). Here the supply of nutrients is likely sufficient to support elevated primary productivity while minimizing the loss of phytoplankton to the ocean. Net CO_2 uptake is most often observed at these moderate FW ages during the spring and summer, as are elevated DO concentrations (Figure 2). Furthermore, despite relatively high CO_2 inputs from the estuary ($[CO_2]_{estuary}$), riverine CO_2 inputs ($[CO_2]_{river}$) were lowest during the summer (Figure 4), resulting in the moderate observed CO_2 fluxes (Table 2). Previous studies have demonstrated this effect in the NewRE and NeuseRE, where phytoplankton biomass was low at short FW age, increasing to a maximum at a FW age of ~10 days (Hall et al., 2013; Peierls et al., 2012). At FW ages above ~10 days, biomass decreased and became dominated by picoplanktonic cyanobacteria. Freshwater discharge and tidal exchange act together to govern the balance between nutrient/OC delivery and the flushing of phytoplankton from the estuary. At a moderate FW age of 2–3 weeks, phytoplankton growth exceeds the rate at which cells are flushed from the estuary, causing a negative air-water CO_2 flux and possible net ecosystem autotrophy. To our knowledge, this is the first study to quantitatively link flushing time with estuarine pCO_2 dynamics, a relationship that demonstrates the strong connection between hydrologic forcing and estuarine biogeochemistry, and supports the modeling results of Laruelle et al. (2017) as well as Maher and Eyre (2012).

While $[CO_2]_{river}$ drives air-water CO_2 exchange in the upper regions of both estuaries, it becomes less significant than $[CO_2]_{estuary}$ further downstream (Figure 6). However, $[CO_2]_{river}$ is only slightly attenuated downstream (Figure 4), likely due to the large amount of time needed for gas exchange to bring a given parcel of water to equilibrium with atmospheric CO_2. When the following average conditions are assumed (typical for the NeuseRE): water depth (H) = 500 cm, k = 8 cm h^{-1}, Revelle factor (R) = 5, [DIC] = 1.2 mM, and $[CO_{2(aq)}]$ = 0.02 mM, the time scale for CO_2 exchange (τ_{CO2}) can be estimated by the following equation (Ito et al., 2004; Jones et al., 2014):

$$\tau_{CO2} = (H/k) \times (1/R) \times \left(\left[DICCO_{2(aq)} \right] \right). \quad (8)$$

Using the values listed previously, equation (8) yields an exchange time of 31 days, which is of similar order as average FW age in the NeuseRE (58 days). If τ_{CO2} were much less than the average FW age, more rapid

decreases in $[CO_2]_{river}$ would be expected. During storm events, FW age is often less than 3 days (Figure S3), but during these periods, wind-driven increases in k will drive concurrent declines in τ_{CO2}. This trade-off between decreasing FW age and τ_{CO2} may affect the fate of inorganic C during storm events. If τ_{CO2} decreases more than FW age, then air-water CO_2 exchange will become increasingly important relative to other loss terms like exchange with the ocean or net ecosystem production. However, if τ_{CO2} decreases less than FW age, the export of inorganic C to the coastal ocean may be enhanced. A comprehensive C budget recently compiled for the NewRE supports this argument, finding that DIC export to the ocean was approximately 2.5 times greater for a wet year than for a dry year, despite comparatively steady DOC export (Crosswell et al., 2017).

4.3. Buffering Effects

As suggested by Hu and Cai (2013), even estuaries with relatively large riverine TA loads may still exhibit a high-salinity MBZ, provided that the DIC of incoming river water is sufficiently high. This appears to be the case in the NewRE, where TA is elevated in the river (Table 1) but high respiration drives DIC:TA toward unity, decreasing the buffering capacity and increasing R. This MBZ is accompanied by a region of relatively high pCO_2 in both estuaries but occurs at a higher salinity in the NewRE (Figure 5 inset). That this region of elevated pCO_2 is colocated with the MBZ in both estuaries is consistent with the concept of buffering; here respiratory inputs of CO_2 drive acidification that cannot be buffered by noncarbonate alkalinity. Despite significant differences in watershed characteristics, poorly buffered MBZs in the upper NewRE and NeuseRE account for a large fraction (~35%) of the surface area of each estuary. These MBZs may influence the fate of DIC in both estuaries, increasing the fraction of DIC that can be exchanged with the atmosphere or assimilated by photoautotrophs in the upper region, before it can be transported downstream as HCO_3^- or CO_3^{2-}. In support of this concept, a recent C budget compiled for the NewRE found that for the time period between July 2014 and July 2015, approximately 24% of the total DIC inputs to the upper estuary were lost to the atmosphere as CO_2 (Crosswell et al., 2017). A similar C budget has not been constructed for the NeuseRE, but we expect that the inorganic C system of this estuary would be similarly sensitive to inputs of DIC.

The variation in location of the MBZ between the NewRE and NeuseRE can be attributed to differences in TA loads between the two rivers (Table 1), which are low in the Neuse River (TA = 349 μmol kg^{-1}) relative to the New River (945 μmol kg^{-1}). This difference may stem from the fact that the geology of the Neuse River watershed is dominated by floodplain alluvium, while that of the New River contains large carbonate mineral deposits (USGS 1993). The dissolution of these carbonate minerals by groundwater contributes to the relatively high DIC in the New River. Additionally, expansive riparian wetlands exist along the tidal freshwater reach immediately upstream of the NewRE but are less common along this portion of the Neuse River (wetlands are sparse along the main body of both estuaries). In effect, respiration of terrestrial OM within the watershed acts in concert with carbonate mineral dissolution to increase DIC:TA in the New River relative to the Neuse River, which in turn causes the MBZ in the NewRE to occur at a higher salinity than in the NeuseRE.

The existence of MBZs in both estuaries suggests that these systems may be sensitive to future acidification stress due to increased atmospheric CO_2 or internal, eutrophication-driven CO_2 inputs, as has been found for other North American estuaries (Cai et al., 2017; Feely et al., 2010; Hu et al., 2015; Wallace et al., 2014). In the U.S. Pacific Northwest estuary, Puget Sound, respiratory CO_2 inputs acted in concert with relatively acidic upwelled ocean water to decrease estuarine pH by ~0.1 units below estimated preindustrial levels (Feely et al., 2010). Hydrogen sulfide oxidation, aerobic respiration, and the open-ocean acidification signal were recently shown to collectively induce significant acidification of the Chesapeake Bay (Cai et al., 2017). Elsewhere, declining alkalinity loads have driven long-term acidification in a set of Texas estuaries (Hu et al., 2015).

In the present study, the magnitude of anthropogenic CO_2-induced acidification on the NewRE and NeuseRE may be estimated by adopting the calculations of Hu and Cai (2013). If we allow a current oceanic TA and DIC end-member to mix conservatively with freshwater (TA and DIC from Table 1), we can then calculate the change in estuarine pH resulting from anthropogenic CO_2 additions to the ocean end-member alone. If atmospheric pCO_2 increases to 800 μatm, a conservative estimate for the year 2100, pH will decrease by a maximum of 0.30 and 0.37 in the NewRE and NeuseRE, respectively (Figure S5). This acidification is

significant, even relative to typical spatial variations in pH on any given sampling date (Figure 2). Interestingly, we calculate that this maximum pH decrease will occur not at the current MBZs (salinity 2–10, Figure 5) but at a higher salinity of 14 and 18 in the NeuseRE and NewRE, respectively. This down-estuary shift in the MBZ with anthropogenic CO_2 additions is already detailed in the literature (Hu & Cai, 2013) and will continue with further increases in atmospheric CO_2. Similar pH decreases could be calculated from expected changes in aerobic (Hu & Cai, 2013; Sunda & Cai, 2012) or anaerobic (Cai et al., 2017) metabolism. Accordingly, factors like eutrophication, ocean acidification, and altered alkalinity loads will likely interact to drive unpredictable pH changes in both the NewRE and NeuseRE. Long-term trends in TA will be particularly important in determining the response of these estuaries to CO_2-induced acidification, as has been demonstrated in the Baltic Sea (Müller et al., 2016). Because these higher-salinity regions of the NeuseRE and particularly NewRE are important for shellfish production, assessments of the vulnerability of these estuaries to future acidification are needed, given that local economies are among the 20% most socially vulnerable to further acidification (Ekstrom et al., 2015).

5. Conclusions

This study contributes to the current understanding that microtidal estuaries are small sources of CO_2 to the atmosphere. We build on previous work by showing that on an annual scale, CO_2 fluxes in the marine-dominated NewRE (15.7–16.9 mmol C m^{-2} d^{-1}) are similar to those in the river-dominated NeuseRE (7.7–17.5 mmol C m^{-2} d^{-1}), both of which are categorized as lagoonal and microtidal. However, these moderate CO_2 fluxes observed in this study are greater than previously reported in the NeuseRE, due to relatively wet and stormy conditions during the study period. We identify a novel relationship between residence time and pCO_2, where pCO_2 is high at low FW age and decreases to a minimum at a FW age of between 2 and 3 weeks. Here nutrient delivery and phytoplankton flushing rates are presumably balanced, likely enhancing net ecosystem productivity. That this pCO_2 minimum occurred at the same FW age in both estuaries indicates that biological drivers are comparable in these hydrodynamically distinct systems. Whether this relationship is universal to all estuaries, or is unique to the NewRE and NeuseRE, remains an open question. Modeling results suggest that riverine inputs of CO_2 ($[CO_2]_{river}$) drove CO_2 fluxes in the river-dominated NeuseRE, while estuarine-generated CO_2 ($[CO_2]_{estuary}$) supported CO_2 fluxes in the marine-dominated NewRE. Finally, a minimum buffering zone (MBZ) occurs in both estuaries, where pCO_2 is particularly sensitive to additional inputs of DIC, and pH is expected to decrease by 0.3 and 0.37 units in the NewRE and NeuseRE, respectively by the year 2100. Differences in the geology and ecology of the respective catchments cause this MBZ to occur in slightly different portions of the NewRE than in the NeuseRE, but anticipated anthropogenic CO_2 additions will cause this pH- and pCO_2-sensitive region to move seaward in the coming decades.

Previous work has shown high spatial and temporal variability in air-water CO_2 exchanges in estuaries. The findings presented in this study emphasize the role that watershed-scale hydrologic factors play in controlling this variability and, thus, the direction and magnitude of CO_2 exchange in microtidal estuaries. Factors associated with a changing climate, like anthropogenic CO_2 emissions, cultural eutrophication, and ocean acidification, which can act in concert with respiratory CO_2 inputs to decrease estuarine pH, may have unpredictable effects on the observed relationships and should be the focus of future investigations.

Acknowledgments

We appreciate the assistance of J. Braddy, H. Walker, B. Abare, K. Rossignol, R. Sloup, and all individuals at VIMS and UNC-IMS who provided support in the field and lab. We thank the many collaborators and technical advisors within the Strategic Environmental Research and Developmental Program—Defense Coastal/Estuarine Research Program (SERDP-DCERP) who have provided insightful comments, data, and general guidance. We are also thankful to S. Cohen of NAVFAC and the Camp Lejeune Environmental Management Division staff. Raw data used in this study, along with most of the relevant calculations, are provided as a compressed file in the supporting information; more detailed inquiries may be directed toward the corresponding author. Data for the NewRE are available online at the following repository maintained by RTI International (https://dcerp.rti.org/login.aspx?ReturnUrl=%2fMARDISHome.aspx). This research was funded by SERDP-DCERP project RC-2245, the North Carolina Department of Environmental Quality (ModMon Program), the Lower Neuse Basin Association, NC Sea Grant, and the UNC Water Resources Research Institute.

References

Akhand, A. A., Akhand, A., Chanda, A., Manna, S., Das, S., Hazra, S., … Wanninkhof, R. (2016). A comparison of CO_2 dynamics and air-water fluxes in a river-dominated estuary and a mangrove-dominated marine estuary. *Geophysical Research Letters*, *43*, 11,726–11,735. https://doi.org/10.1002/2016GL070716

Alber, M., & Sheldon, J. E. (1999). Use of a date-specific method to examine variability in the flushing times of Georgia estuaries. *Estuarine, Coastal and Shelf Science*, *49*(4), 469–482. https://doi.org/10.1006/ecss.1999.0515

Barton, A., Hales, B., Waldbusser, G. G., Langdon, C., & Feely, R. A. (2012). The Pacific oyster, *Crassostrea gigas*, shows negative correlation to naturally elevated carbon dioxide levels: Implications for near-term ocean acidification effects. *Limnology and Oceanography*, *57*, 698–710. https://doi.org/10.4319/lo.2012.57.3.0698

Bauer, J. E., Cai, W.-J., Raymond, P. A., Bianchi, T. S., Hopkinson, C. S., & Regnier, P. G. (2013). The changing carbon cycle of the coastal ocean. *Nature*, *504*(7478), 61–70. https://doi.org/10.1038/nature12857

Beman, J. M., Chow, C., King, A. L., Feng, Y., & Fuhrman, J. A. (2010). Global declines in oceanic nitrification rates as a consequence of ocean acidification. *Proceedings of the National Academy of Sciences of the United States of America*, *108*, 208–213. https://doi.org/10.1073/pnas.1011053108/-/DCSupplemental.www.pnas.org/cgi/doi/10.1073/pnas.1011053108

Borges, A. V., & Abril, G. (2011). Carbon dioxide and methane dynamics in estuaries. In E. Wolanski & D. McLusky (Eds.), *Treatise on estuarine and coastal science* (Vol. 5, pp. 119–161). Waltham: Academic Press. https://doi.org/10.1016/B978-0-12-374711-2.00504-0.

Borges, A. V., & Abril, G. (2012). Carbon Dioxide and Methane Dynamics in Estuaries. In *Treatise on Estuarine and Coastal Science* (Vol. 5). Elsevier Inc. https://doi.org/10.1016/B978-0-12-374711-2.00504-0

Borges, A. V., Delille, B., Schiettecatte, L., Gazeau, F., Abril, G., & Frankignoulle, M. (2004). Gas transfer velocities of CO_2 in three European estuaries (Randers Fjord, Scheldt, and Thames). *Limnology and Oceanography*, *49*(5), 1630–1641. https://doi.org/10.4319/lo.2004.49.5.1630

Borges, A. V., Vanderborght, J.-P., Schiettecatte, L., Gazeau, F., Ferron-Smith, S., Delille, B., & Frankignoulle, M. (2004). Variability of the gas transfer velocity of CO_2 in a macrotidal estuary (the Scheldt). *Estuaries*, *27*(4), 593–603. https://doi.org/10.1007/BF02907647

Boyer, J. N., Christian, R. R., & Stanleyl, D. W. (1993). Patterns of phytoplankton primary productivity in the Neuse River Estuary, North Carolina, USA. *Marine Ecology Progress Series*, *97*, 287–297. https://doi.org/10.3354/meps097287

Cai, W.-J. (2011). Estuarine and coastal ocean carbon paradox: CO_2 sinks or sites of terrestrial carbon incineration? *Annual Review of Marine Science*, *3*(1), 123–145. https://doi.org/10.1146/annurev-marine-120709-142723

Cai, W.-J., Hu, X., Huang, W.-J., Murrell, M. C., Lehrter, J. C., Lohrenz, S. E., … Gong, G.-C. (2011). Acidification of subsurface coastal waters enhanced by eutrophication. *Nature Geoscience*, *4*(11), 766–770. https://doi.org/10.1038/ngeo1297

Cai, W.-J., Huang, W.-J., Luther, G. W., Pierrot, D., Li, M., Testa, J., … Kemp, W. M. (2017). Redox reactions and weak buffering capacity lead to acidification in the Chesapeake Bay. *Nature Communications*, *8*(1), 369. https://doi.org/10.1038/s41467-017-00417-7

Cai, W.-J., & Wang, Y. (1998). The chemistry, fluxes, and sources of carbon dioxide in the estuarine waters of the Satilla and Altamaha Rivers, Georgia. *Limnology and Oceanography*, *43*(4), 657–668. https://doi.org/10.4319/lo.1998.43.4.0657

Call, M., Maher, D. T., Santos, I. R., Ruiz-Halpern, S., Mangion, P., Sanders, C. J., … Eyre, B. D. (2015). Spatial and temporal variability of carbon dioxide and methane fluxes over semi-diurnal and spring–neap–spring timescales in a mangrove creek. *Geochimica et Cosmochimica Acta*, *150*, 211–225. https://doi.org/10.1016/j.gca.2014.11.023

Catalán, N., Marcé, R., Kothawala, D. N., & Tranvik, L. J. (2016). Organic carbon decomposition rates controlled by water retention time across inland waters. *Nature Geoscience*, *9*(7), 501–504. https://doi.org/10.1038/ngeo2720

Chen, C.-T. A., & Borges, A. V. (2009). Reconciling opposing views on carbon cycling in the coastal ocean: Continental shelves as sinks and near-shore ecosystems as sources of atmospheric CO_2. *Deep Sea Research, Part II*, *56*, 554–577. https://doi.org/10.1016/j.dsr2.2008.12.009

Chen, C.-T. A., Huang, T. H., Chen, Y. C., Bai, Y., He, X., & Kang, Y. (2013). Air-sea exchanges of CO_2 in the world's coastal seas. *Biogeosciences*, *10*(10), 6509–6544. https://doi.org/10.5194/bg-10-6509-2013

Crosswell, J. R., Anderson, I. C., Stanhope, J. W., van Dam, B., Brush, M. J., Ensign, S., … Paerl, H. W. (2017). Carbon budget of a shallow, lagoonal estuary: Transformations and source-sink dynamics along the river-estuary-ocean continuum. *Limnology and Oceanography*, *62*, S29–S45. https://doi.org/10.1002/lno.10631

Crosswell, J. R., Wetz, M. S., Hales, B., & Paerl, H. W. (2012). Air-water CO_2 fluxes in the microtidal Neuse River Estuary, North Carolina. *Journal of Geophysical Research*, *117*, C08017. https://doi.org/10.1029/2012JC007925

Crosswell, J. R., Wetz, M. S., Hales, B., & Paerl, H. W. (2014). Extensive CO_2 emissions from shallow coastal waters during passage of Hurricane Irene (August 2011) over the Mid-Atlantic Coast of the U.S.A. *Limnology and Oceanography*, *59*(5), 1651–1665. https://doi.org/10.4319/lo.2014.59.5.1651

Currin, C., Davis, J., Cowart, B. L., Malhotra, A., & Fonseca, M. (2015). Shoreline change in the New River Estuary, North Carolina: Rates and consequences. *Journal of Coastal Research*, *315*, 1069–1077. https://doi.org/10.2112/JCOASTRES-D-14-00127.1

Dhillon, G. S., & Inamdar, S. (2013). Extreme storms and changes in particulate and dissolved organic carbon in runoff: Entering uncharted waters? *Geophysical Research Letters*, *40*, 1322–1327. https://doi.org/10.1002/grl.50306

Dickson, A. G., & Millero, F. J. (1987). A comparison of the equilibrium constants for the dissociation of carbonic acid in seawater media. *Deep Sea Research*, *34*(10), 1733–1743. https://doi.org/10.1016/0198-0149(87)90021-5

Dodd, L. F., Grabowski, J. H., Piehler, M. F., Westfield, I., & Ries, J. B. (2015). Ocean acidification impairs crab foraging behaviour. *Proceedings of the Royal Society B: Biological Sciences*, *282*(1810), 20150333. https://doi.org/10.1098/rspb.2015.0333

Doney, S. C., Fabry, V. J., Feely, R. A., & Kleypas, J. A. (2009). Ocean Acidification: The Other CO_2 Problem. *Annual Review of Marine Science*, *1*(1), 169–192. https://doi.org/10.1146/annurev.marine.010908.163834

Drupp, P., De Carlo, E. H., Mackenzie, F. T., Bienfang, P., & Sabine, C. L. (2011). Nutrient inputs, phytoplankton response, and CO_2 variations in a semi-enclosed subtropical embayment, Kaneohe BayHawaii. *Aquatic Geochemistry*, *17*, 473–498. https://doi.org/10.1007/s10498-010-9115-y

Egleston, E. S., Sabine, C. L., & Morel, F. M. M. (2010). Revelle revisited: Buffer factors that quantify the response of ocean chemistry to changes in DIC and alkalinity. *Global Biogeochemical Cycles*, *24*, GB1002. https://doi.org/10.1029/2008GB003407

Ekstrom, J. A., Suatoni, L., Cooley, S. R., Pendleton, L. H., Waldbusser, G. G., Cinner, J. E., … Portela, R. (2015). Vulnerability and adaptation of US shellfisheries to ocean acidification. *Nature Climate Change*, *5*(3), 207–214. https://doi.org/10.1038/nclimate2508

Ensign, S., Siporin, K., Piehler, M., Doyle, M., & Leonard, L. (2013). Hydrologic versus biogeochemical controls of denitrification in tidal freshwater wetlands. *Estuaries and Coasts*, *36*(3), 519–532. https://doi.org/10.1007/s12237-012-9491-1

Ensign, S. H., Halls, J. N., & Mallin, M. A. (2004). Application of digital bathymetry data in an analysis of flushing times of two large estuaries. *Computers and Geosciences*, *30*, 501–511. https://doi.org/10.1016/j.cageo.2004.03.015

Evans, W., Hales, B., & Strutton, P. G. (2013). pCO_2 distributions and air–water CO_2 fluxes in the Columbia River estuary. *Estuarine, Coastal and Shelf Science*, *117*, 260–272. https://doi.org/10.1016/j.ecss.2012.12.003

Fear, J. M., Paerl, H. W., & Braddy, J. S. (2007). Importance of submarine groundwater discharge as a source of nutrients for the Neuse River Estuary, North Carolina. *Estuaries and Coasts*, *30*, 1027–1033. https://doi.org/10.1007/BF02841393

Feely, R. A., Alin, S. R., Newton, J., Sabine, C. L., Warner, M., Devol, A., … Maloy, C. (2010). The combined effects of ocean acidification, mixing, and respiration on pH and carbonate saturation in an urbanized estuary. *Estuarine, Coastal and Shelf Science*, *88*, 442–449. https://doi.org/10.1016/j.ecss.2010.05.004

Flecha, S., Huertas, I. E., Navarro, G., Morris, E. P., & Ruiz, J. (2015). Air–water CO_2 fluxes in a highly heterotrophic estuary. *Estuaries and Coasts*, *38*(6), 2295–2309. https://doi.org/10.1007/s12237-014-9923-1

Frankignoulle, M., Abril, G., Borges, A., Bourge, I., Canon, C., Delille, B., … Theate, J. (1998). Carbon dioxide emission from European estuaries. *Science*, *282*(5388), 434–436. https://doi.org/10.1126/science.282.5388.434

Frankignoulle, M., & Borges, A. V. (2002). Direct and indirect pCO_2 measurements in a wide range of pCO_2 and salinity values (the Scheldt Estuary). *Aquatic Geochemistry*, *7*, 267–273.

Guo, X., Dai, M., Zhai, W., Cai, W.-J., & Chen, B. (2009). CO_2 flux and seasonal variability in a large subtropical estuarine system, the Pearl River Estuary, China. *Journal of Geophysical Research*, *114*, GO3013. https://doi.org/10.1029/2008JG000905

Hall, N. S., Paerl, H. W., Peierls, B. L., Whipple, A. C., & Rossignol, K. L. (2013). Effects of climatic variability on phytoplankton biomass and community structure in the eutrophic, microtidal, New River Estuary, North Carolina, USA. *Estuarine, Coastal and Shelf Science*, *117*, 70–82. https://doi.org/10.1016/j.ecss.2012.10.004

Hall, N. S., Whipple, A. C., & Paerl, H. W. (2015). Vertical spatio-temporal patterns of phytoplankton due to migration behaviors in two shallow, microtidal estuaries: Influence on phytoplankton function and structure. *Estuarine, Coastal and Shelf Science*, *162*, 7–21. https://doi.org/10.1016/j.ecss.2015.03.032

Ho, D. T., Law, C. S., Smith, M. J., Schlosser, P., Harvey, M., & Hill, P. (2006). Measurements of air-sea gas exchange at high wind speeds in the Southern Ocean: Implications for global parameterizations. *Geophysical Research Letters*, *33*, L16611. https://doi.org/10.1029/2006GL026817

Hobbie, J. E. (Ed.) (2000). *Estuarine science: A synthetic approach to research and practice* (p. 539). Washington, DC: Island Press.

Hofmann, G. E., Barry, J. P., Edmunds, P. J., Gates, R. D., Hutchins, D. A., Klinger, T., & Sewell, M. A. (2010). The effect of ocean acidification on calcifying organisms in marine ecosystems: An organism-to-ecosystem perspective. *Annual Review of Ecology, Evolution, and Systematics*, *41*, 127–147. https://doi.org/10.1146/annurev.ecolsys.110308.120227

Hotchkiss, E. R., Hall, R. O. Jr., Sponseller, R. A., Butman, D., Klaminder, J., Laudon, H., … Karlsson, J. (2015). Sources of and processes controlling CO_2 emissions change with the size of streams and rivers. *Nature Geoscience*, *8*(9), 696–699. https://doi.org/10.1038/ngeo2507

Hu, X., & Cai, W. J. (2013). Estuarine acidification and minimum buffer zone—A conceptual study. *Geophysical Research Letters*, *40*, 5176–5181. https://doi.org/10.1002/grl.51000

Hu, X., Pollack, J. B., McCutcheon, M. R., Montagna, P. A., & Ouyang, Z. (2015). Long-term alkalinity decrease and acidification of estuaries in northwestern Gulf of Mexico. *Environmental Science & Technology*, *49*(6), 3401–3409. https://doi.org/10.1021/es505945p

Huesemann, M. H., Skillman, A. D., & Crecelius, E. A. (2002). The inhibition of marine nitrification by ocean disposal of carbon dioxide. *Marine Pollution Bulletin*, *44*(2), 142–148. https://doi.org/10.1016/S0025-326X(01)00194-1

Hunt, C. W., Salisbury, J. E., Vandemark, D., & McGillis, W. (2011). Contrasting Carbon Dioxide Inputs and Exchange in Three Adjacent New England Estuaries. *Estuaries and Coasts*, *34*(1), 68–77. https://doi.org/10.1007/s12237-010-9299-9

Hunt, C. W., Salisbury, J. E., & Vandemark, D. (2013). CO_2 input dynamics and air–sea exchange in a large New England estuary. *Estuaries and Coasts*, *37*(5), 1078–1091. https://doi.org/10.1007/s12237-013-9749-2

Ito, T., Marshall, J., & Follows, M. (2004). What controls the uptake of transient tracers in the Southern Ocean? *Global Biogeochemical Cycles*, *18*, GB2021. https://doi.org/10.1029/2003GB002103

Jeffrey, L. C., Maher, D. T., Santos, I. R., McMahon, A., & Tait, D. R. (2016). Groundwater, acid and carbon dioxide dynamics along a coastal wetland, lake and estuary continuum. *Estuaries and Coasts*, *39*(5), 1325–1344. https://doi.org/10.1007/s12237-016-0099-8

Jiang, L.-Q., Cai, W.-J., & Wang, Y. (2008). A comparative study of carbon dioxide degassing in river- and marine-dominated estuaries. *Limnology and Oceanography*, *53*, 2603–2615. https://doi.org/10.4319/lo.2008.53.6.2603

Joesoef, A., Huang, W. J., Gao, Y., & Cai, W.-J. (2015). Air-water fluxes and sources of carbon dioxide in the Delaware Estuary: Spatial and seasonal variability. *Biogeosciences*, *12*(20), 6085–6101. https://doi.org/10.5194/bg-12-6085-2015

Jones, D. C., Ito, T., Takano, Y., & Hsu, W. C. (2014). Spatial and seasonal variability of the air-sea equilibration timescale of carbon dioxide. *Global Biogeochemical Cycles*, *28*, 1163–1178. https://doi.org/10.1002/2014GB004813

Kennish, M., & Paerl, H. W. (2010). *Coastal lagoons: Critical habitats of environmental change*, *CRC Marine Science Series*. Boca Raton, FL: CRC Press. https://doi.org/10.1201/EBK1420088304

Koné, Y. J. M., Abril, G., Kouadio, K. N., Delille, B., & Borges, A. V. (2009). Seasonal variability of carbon dioxide in the rivers and lagoons of Ivory Coast (West Africa). *Estuaries and Coasts*, *32*, 246–260. https://doi.org/10.1007/s12237-008-9121-0

Langley, J. A., & Megonigal, J. P. (2010). Ecosystem response to elevated CO_2 levels limited by nitrogen-induced plant species shift. *Nature*, *466*, 96–99. https://doi.org/10.1038/nature09176

Laruelle, G. G., Dürr, H. H., Lauerwald, R., Hartmann, J., Slomp, C. P., Goossens, N., & Regnier, P. A. G. (2013). Global multi-scale segmentation of continental and coastal waters from the watersheds to the continental margins. *Hydrology and Earth System Sciences*, *17*(5), 2029–2051. https://doi.org/10.5194/hess-17-2029-2013

Laruelle, G. G., Dürr, H. H., Slomp, C. P., & Borges, A. V. (2010). Evaluation of sinks and sources of CO_2 in the global coastal ocean using a spatially-explicit typology of estuaries and continental shelves. *Geophysical Research Letters*, *37*, L15607. https://doi.org/10.1029/2010GL043691

Laruelle, G. G., Goossens, N., Arndt, S., Cai, W.-J., & Regnier, P. (2017). Air-water CO_2 evasion from U.S. East Coast estuaries. *Biogeosciences*, *14*, 1–54. https://doi.org/10.5194/bg-2016-278

Leung, J. Y. S., Russell, B. D., Connell, S. D., Ng, J. C. Y., & Lo, M. M. Y. (2015). Acid dulls the senses: Impaired locomotion and foraging performance in a marine mollusk. *Animal Behaviour*, *106*, 223–229. https://doi.org/10.1016/j.anbehav.2015.06.004

Lewis, E., & Wallace, D. (1998). In C.D.I.A. Center (Ed.), *Program developed for CO_2 system calculations*. Oak Ridge, TN: Carbon Dioxide Information Analysis Center.

Litaker, R. W., Tester, P. A., Duke, C. S., Kenney, B. E., Pinckney, J. L., & Ramus, J. (2002). Seasonal niche strategy of the bloom-forming dinoflagellate *Heterocapsa triquetra*. *Marine Ecology Progress Series*, *232*, 45–62. https://doi.org/10.3354/meps232045

Luettich, R. A., Reynolds-Fleming, J. V., McNinch, J. E., & Buzzelli, C. P. (2000). Circulation characteristics of the Neuse River Estuary, North Carolina. *Estuaries*, *23*(2), 392–399.

Macklin, P. A., Maher, D. T., & Santos, I. R. (2014). Estuarine canal estate waters: Hotspots of CO_2 outgassing driven by enhanced groundwater discharge? *Marine Chemistry*, *167*, 82–92. https://doi.org/10.1016/j.marchem.2014.08.002

Maher, D. T., Cowley, K., Santos, I. R., Macklin, P., & Eyre, B. D. (2015). Methane and carbon dioxide dynamics in a subtropical estuary over a diel cycle: Insights from automated in situ radioactive and stable isotope measurements. *Marine Chemistry*, *168*, 69–79. https://doi.org/10.1016/j.marchem.2014.10.017

Maher, D. T., & Eyre, B. D. (2012). Carbon budgets for three autotrophic Australian estuaries: Implications for global estimates of the coastal air-water CO_2 flux. *Global Biogeochemical Cycles*, *26*, GB1032. https://doi.org/10.1029/2011GB004075

Mallin, M., Paerl, H. W., Rudek, J., & Bates, P. (1993). Regulation of estuarine primary production by watershed rainfall and river flow. *Marine Ecology Progress Series*, *93*, 199–203. https://doi.org/10.3354/meps093199

Mallin, M. A., McIver, M. R., Wells, H. A., Parsons, D. C., & Johnson, V. L. (2005). Reversal of eutrophication following sewage treatment upgrades in the New River Estuary, North Carolina. *Estuaries*, *28*, 750–760. https://doi.org/10.1007/BF02732912

Millero, F. J. (2013). *Chemical oceanography* (4th ed.). Boca Raton, FL: CRC Press.

Mørk, E. T., Sejr, M., Stæhr, P. A., & Sørensen, L. L. (2016). Temporal variability of air-sea CO_2 exchange in a low-emission estuary. *Estuarine, Coastal and Shelf Science*, *176*, 1–11. https://doi.org/10.1016/j.ecss.2016.03.022

Mozdzer, T. J., & Megonigal, J. P. (2012). Jack-and-master trait responses to elevated CO_2 and N: A comparison of native and introduced *Phragmites australis*. *PLoS One*, *7*, e42794. https://doi.org/10.1371/journal.pone.0042794

Müller, J. D., Schneider, B., & Rehder, G. (2016). Long-term alkalinity trends in the Baltic Sea and their implications for CO_2-induced acidification. *Limnology and Oceanography*, *61*(6), 1984–2002. https://doi.org/10.1002/lno.10349

Najjar, R. G., Pyke, C. R., Adams, M. B., Breitburg, D., Hershner, C., Kemp, M., … Wood, R. (2010). Potential climate-change impacts on the Chesapeake Bay. *Estuarine, Coastal and Shelf Science*, *86*, 1–20. https://doi.org/10.1016/j.ecss.2009.09.026

Neubauer, S. C., & Anderson, I. C. (2003). Transport of dissolved inorganic carbon from a tidal freshwater marsh to the York River estuary. *Limnology and Oceanography*, *48*(1), 299–307. https://doi.org/10.4319/lo.2003.48.1.0299

Null, K. A., Corbett, D. R., DeMaster, D. J., Burkholder, J. M., Thomas, C. J., & Reed, R. E. (2011). Porewater advection of ammonium into the Neuse River Estuary, North Carolina, USA. *Estuarine, Coastal and Shelf Science*, *95*, 314–325. https://doi.org/10.1016/j.ecss.2011.09.016

Paerl, H. W., Hall, N. S., Peierls, B. L., Rossignol, K. L., & Joyner, A. R. (2014). Hydrologic variability and its control of phytoplankton community structure and function in two shallow, coastal, lagoonal ecosystems: The Neuse and New River Estuaries, North Carolina, USA. *Estuaries and Coasts*, *37*(S1), 31–45. https://doi.org/10.1007/s12237-013-9686-0

Paerl, H. W., Pinckney, J., Fear, J., & Peierls, B. L. (1998). Ecosystem responses to internal and watershed organic matter loading: Consequences for hypoxia in the eutrophying Neuse River Estuary, North Carolina, USA. *Marine Ecology Progress Series*, *166*, 17–25. https://doi.org/10.3354/meps166017

Paerl, H. W., Valdes, L. M., Joyner, A. R., & Winkelmann, V. (2007). Phytoplankton indicators of ecological change in the nutrient and climatically-impacted Neuse River-Pamlico Sound system, North Carolina. *Ecological Applications*, *17*(5), 88–101.

Peierls, B. L., Hall, N. S., & Paerl, H. W. (2012). Non-monotonic responses of phytoplankton biomass accumulation to hydrologic variability: A comparison of two coastal plain North Carolina estuaries. *Estuaries and Coasts*, *35*, 1376–1392. https://doi.org/10.1007/s12237-012-9547-2

Pendleton, L. H. (Ed.) (2008). *The economic and market value of coasts and estuaries: What's at stake?* Arlington, VA: Restore Am. Estuaries.

Prytherch, J., Yelland, M. J., Pascal, R. W., Moat, B. I., Skjelvan, I., & Srokosz, M. A. (2010). Open ocean gas transfer velocity derived from long-term direct measurements of the CO_2 flux. *Geophysical Research Letters*, *37*, L23607. https://doi.org/10.1029/2010GL045597

Raymond, P. A., & Cole, J. J. (2001). Gas exchange in rivers and estuaries: Choosing a gas transfer velocity. *Estuaries*, *24*(2), 312–317. https://doi.org/10.2307/1352954

Regnier, P., Friedlingstein, P., Ciais, P., Mackenzie, F. T., Gruber, N., Janssens, I. A., … Thullner, M. (2013). Anthropogenic perturbation of the carbon fluxes from land to ocean. *Nature Geoscience*, *6*(8), 597–607. https://doi.org/10.1038/ngeo1830

Reynolds-Fleming, J. V., Fleming, J. G., & Luettich, R. A. (2002). Portable, autonomous vertical profiler for estuarine applications. *Estuaries*, *25*(1), 142–147. https://doi.org/10.1007/BF02696058

Rosentreter, J. A., Maher, D. T., Ho, D. T., Call, M., Barr, J. G., & Eyre, B. D. (2016). Spatial and temporal variability of CO_2 and CH_4 gas transfer velocities and quantification of the CH_4 microbubble flux in mangrove dominated estuaries. *Limnology and Oceanography*, *62*(2), 561–578 . https://doi.org/10.1002/lno.10444

Ruiz-Halpern, S., Maher, D. T., Santos, I. R., & Eyre, B. D. (2015). High CO_2 evasion during floods in an Australian subtropical estuary downstream from a modified acidic floodplain wetland. *Limnology and Oceanography*, *60*(1), 42–56. https://doi.org/10.1002/lno.10004

Santos, I. R., Maher, D. T., & Eyre, B. D. (2012). Coupling automated radon and carbon dioxide measurements in coastal waters. *Environmental Science & Technology*, *46*(14), 7685–7691. https://doi.org/10.1021/es301961b

Santos, I. R., Peterson, R. N., Eyre, B. D., & Burnett, W. C. (2010). Significant lateral inputs of fresh groundwater into a stratified tropical estuary: Evidence from radon and radium isotopes. *Marine Chemistry*, *121*, 37–48. https://doi.org/10.1016/j.marchem.2010.03.003

Sierra, C. A., Müller, M., Metzler, H., Manzoni, S., & Trumbore, S. E. (2017). The muddle of ages, turnover, transit, and residence times in the carbon cycle. *Global Change Biology*, *23*(5), 1763–1773. https://doi.org/10.1111/gcb.13556

Smethie, W. M., Takahashi, T., & Chipman, D. W. (1985). Gas exchange and CO_2 flux in the tropical Atlantic Ocean determined from ^{222}Rn and pCO_2 measurements. *Journal of Geophysical Research*, *90*(C4), 7005–7022. https://doi.org/10.1029/JC090iC04p07005

Sunda, W. G., & Cai, W.-J. (2012). Eutrophication induced CO_2-acidification of subsurface coastal waters: Interactive effects of temperature, salinity, and atmospheric pCO_2. *Environmental Science & Technology*, *46*(19), 10651–10659. https://doi.org/10.1021/es300626f

Upstill-Goddard, R. C. (2006). Air–sea gas exchange in the coastal zone. *Estuarine, Coastal and Shelf Science*, *70*(3), 388–404. https://doi.org/10.1016/j.ecss.2006.05.043

USGS (1993). *Hydrogeologic framework of U.S. Marine Corps Base at Camp Lejeune, North Carolina*. Washington DC: United States Geological Survey. Retrieved from https://pubs.er.usgs.gov/publication/wri934049

Vachon, D., & del Giorgio, P. A. (2014). Whole-lake CO_2 dynamics in response to storm events in two morphologically different lakes. *Ecosystems*, *17*(8), 1338–1353. https://doi.org/10.1007/s10021-014-9799-8

Von Korff, B. H., Piehler, M. F., & Ensign, S. H. (2014). Comparison of Denitrification Between River Channels and Their Adjoining Tidal Freshwater Wetlands. *Wetlands*, *34*(6), 1047–1060. https://doi.org/10.1007/s13157-014-0545-y

Wallace, R. B., Baumann, H., Grear, J. S., Aller, R. C., & Gobler, C. J. (2014). Coastal ocean acidification: The other eutrophication problem. *Estuarine, Coastal and Shelf Science*, *148*, 1–13. https://doi.org/10.1016/j.ecss.2014.05.027

Wang, Z. A., & Cai, W.-J. (2004). Carbon dioxide degassing and inorganic carbon export from a marsh-dominated estuary (the Duplin River): A marsh CO_2 pump. *Limnology and Oceanography*, *49*(2), 341–354. https://doi.org/10.4319/lo.2004.49.2.0341

Wanninkhof, R., Asher, W. E., Ho, D. T., Sweeney, C., & McGillis, W. R. (2009). Advances in quantifying air-sea gas exchange and environmental forcing. *Annual Review of Marine Science*, *1*, 213–244. https://doi.org/10.1146/annurev.marine.010908.163742

Wanninkhof, R., & Mcgillis, W. R. (1999). A cubic relationship between air-sea CO_2 exchange and wind speed. *Geophysical Research Letters*, *26*(13), 1889–1892. https://doi.org/10.1029/1999GL900363

Weiss, R. F. (1974). Carbon dioxide in water and seawater: The solubility of a non-ideal gas. *Marine Chemistry*, *2*(3), 203–215. https://doi.org/10.1016/0304-4203(74)90015-2

Wetz, M. S., & Yoskowitz, D. W. (2013). An "extreme" future for estuaries? Effects of extreme climatic events on estuarine water quality and ecology. *Marine Pollution Bulletin*, *69*(1-2), 7–18. https://doi.org/10.1016/j.marpolbul.2013.01.020

Woolf, D. K. (2005). Parametrization of gas transfer velocities and sea-state-dependent wave breaking. *Tellus Series B: Chemical and Physical Meteorology*, *57*, 87–94. https://doi.org/10.1111/j.1600-0889.2005.00139.x

Yao, G., Gao, Q., Wang, Z., Huang, X., He, T., Zhang, Y., … Ding, J. (2007). Dynamics of CO_2 partial pressure and CO_2 outgassing in the lower reaches of the Xijiang River, a subtropical monsoon river in China. *Science of the Total Environment*, *376*, 255–266. https://doi.org/10.1016/j.scitotenv.2007.01.080

Zhai, W., Dai, M., Cai, W.-J., Wang, Y., & Wang, Z. (2005). High partial pressure of CO_2 and its maintaining mechanism in a subtropical estuary: The Pearl River estuary, China. *Marine Chemistry*, *93*, 21–32. https://doi.org/10.1016/j.marchem.2004.07.003

Zimmerman, R. C., Hill, V. J., & Gallegos, C. L. (2015). Predicting effects of ocean warming, acidification, and water quality on Chesapeake region eelgrass. *Limnology and Oceanography*, *60*(5), 1781–1804. https://doi.org/10.1002/lno.10139